DOI: 10.1002/ejoc.201201437

Diphosphonylation of Aromatic Diazaheterocycles and Theoretical Rationalization of Product Yields

Ann De Blieck,[a] Saron Catak,[b] Wouter Debrouwer,[a] Józef Drabowicz,[c] Karen Hemelsoet,[b] Toon Verstraelen,[b] Michel Waroquier,[b] Veronique Van Speybroeck,*[b] and Christian V. Stevens*[a]

Keywords: Phosphonylation / Nitrogen heterocycles / Nucleophilic addition / Density functional calculations

Diphosphonylated diazaheterocyclic compounds were synthesized in a one-step reaction by using dimethyl trimethylsilyl phosphite (DMPTMS) under acidic conditions. The reaction of DMPTMS with 1,5-naphthyridine yielded the corresponding diphosphonylated product through a tandem 1,4–1,2 addition under microwave conditions. This tandem 1,4–1,2 addition was also evaluated for other substrates, namely, 1,10-phenanthroline, 1,7-phenanthroline and 4,7-phenanthroline. Reactions under reflux and microwave conditions were compared. 1,5-Naphthyridine and the phenanthroline derived substrates are less reactive than previously investigated quinolines. The experimental trends in reactivity were rationalized by means of theoretical calculations. The intrinsic properties, such as aromaticity and proton affinities, showed distinct differences for the various substrates. Furthermore, the calculated free energies of activation for the rate-determining step of the tandem addition reaction enabled us to rationalize the differences in product yields. Both the theoretical and the experimental results show the substantial influence of the position of the nitrogen atoms in the (poly)aromatic compounds on the reaction outcome.

Introduction

The importance of azaheterocyclic phosphonates in synthetic, agrochemical and medicinal chemistry has been well-documented throughout the years.[1] Simple dialkyl phosphonates bearing a 2-pyridyl moiety are widely used as corrosion inhibitors, dispersing and emulsifying agents, antistatic and lubricant additives in various technologies.[2] In addition, phosphonylated pyridines are also known as potent insecticides,[3a] fungicides[3b–3c] and herbicides.[3d] Recently, the antiproliferative and antiplatelet-activating factor (anti-PAF) properties of pyridin-3-ylphosphonate **1** have been reported,[4a–4b] and the quinolylphosphonic acid derivatives **2** and **3** were found to possess potent antagonistic activity against AMPA receptors; AMPA [2-amino-3-(3-hydroxy-5-methylisoxazol-4-yl)propanoic acid] is an agonist that mimics the important neurotransmitter glutamate (Figure 1).

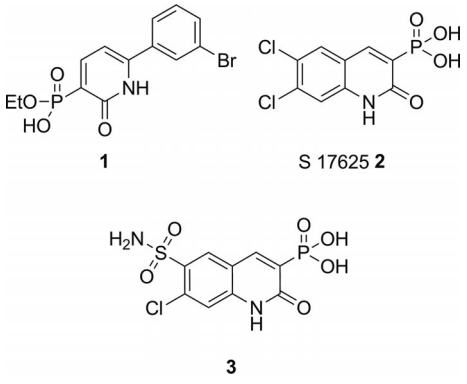

Figure 1. Biologically active phosphonates and phosphonic acids.

Consequently, phosphonylated azaheterocycles gained a lot of interest, and the number of synthetic pathways to these compounds has increased significantly over the years.[5] Nevertheless, in spite of the possible interesting biological activities of azaheterocyclic diphosphonates and diphosphonic acids, no synthetic routes are known towards diphosphonylated diazaheterocycles that use direct phosphonylation to introduce the two phosphorus moieties. Known literature methods use different activation tech-

[a] Department of Sustainable Organic Chemistry and Technology, Faculty of Bioscience Engineering, Ghent University, Coupure Links 653, 9000 Ghent, Belgium
Fax: +32-9-2646221
E-mail: Chris.Stevens@UGent.be
Homepage: www.SynBioC.UGent.be
[b] Center for Molecular Modeling, Ghent University, Technologiepark 903, 9052 Zwijnaarde, Belgium, Member of the QCMM Alliance Ghent-Brussels
Fax: +32-9-2646697
E-mail: Veronique.Vanspeybroeck@UGent.be
Homepage: molmod.UGent.be
[c] Center of Molecular and Macromolecular Studies, Polish Academy of Sciences, Department of Heteroorganic Chemistry, 90-363 Łódź, Sienkiewicza 112, Poland
Fax: +48-42-6847126
E-mail: draj@bilbo.cbmm.lodz.pl
Supporting information for this article is available on the WWW under http://dx.doi.org/10.1002/ejoc.201201437.

niques to facilitate the nucleophilic attack of the phosphorus group. After phosphite addition, the aromaticity is often restored before the isolation of the end product from the reaction mixture. Through a Reissert-type reaction with different sulfonyl or acyl chlorides as *N*-sulfonating or *N*-acylating agent, respectively, 1,8-naphthyridine and 1,7-phenanthroline can be activated towards the attack of the phosphorus nucleophile.[6a–6c] Treatment of the different activated substrates with trialkyl phosphite in the presence of sodium iodide delivered monophosphonylated 1,2-adducts. For 1,7-phenanthroline, the formation of a 1,4-adduct was also observed. On the other hand, Barycki used an excess of diisopropyl phosphite in the presence of metallic sodium, which caused an unexpected nucleophilic substitution in *o*-phthalazine. Subsequent acidic hydrolysis delivered 1-phthalazine phosphonic acid as a crystalline compound in 24% yield.[7] Other activation methods comprise the use of methyl iodide followed by the addition of trimethyl phosphite or dimethyl sodiophosphonate to prepare α- or γ-phosphonylated 1,7-phenanthroline and α- or γ-phosphonylated 1,5- or 1,8-naphthyridine in moderate-to-good yields.[8] Besides this regioselective 1,2- or 1,4-addition of phosphites to azaheterocycles, Takeuchi et al. also reported the synthesis of regio- and stereoisomeric diphosphonates from 4,7-phenanthroline from their corresponding *N*-phenanthrolinium salts. The isomeric adducts were separated through column chromatography.[6c,9]

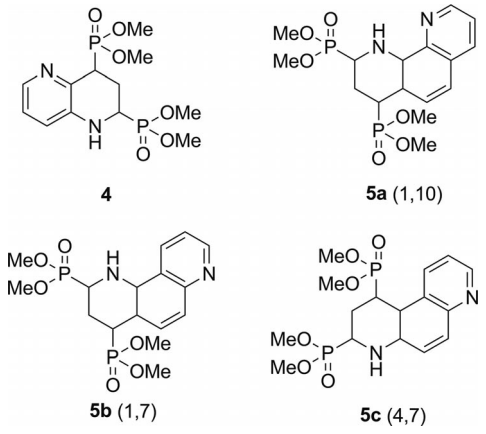

Figure 2. Diphosphonylated 1,5-naphthyridine **4** and phenanthrolines **5a**–**c**.

Following our previous studies on the tandem 1,4–1,2-addition of phosphorus nucleophiles [silylated dialkyl phosphite (DAPTMS) and trialkyl phosphite (TAP)] to α,β-unsaturated aldimines,[10a–10b] hydrazones,[10c] quinolines and acridine,[10d] a new straightforward strategy was elaborated, which led to diphosphonylated 1,5-naphthyridine **1** and phenanthrolines **5a**–**c** (Figure 2).

Results and Discussion

1. Results

In previous work, the intermediates formed during the addition could be spectroscopically determined;[10a] however, during the course of this work, similar intermediates (**8, 9** and **10**) in the proposed reaction mechanism shown in Scheme 1 could not be isolated or structurally determined. It is noteworthy that the addition proceeds despite the break-up of the aromatic stabilization. Dimethyl trimethylsilyl phosphite was used as a phosphorus nucleophile, based on the synthesis of α-aminophosphonates by Afarinkia and co-workers.[11] Afarinkia presented silylated phosphites as excellent mild phosphonylation agents owing to the more nucleophilic $\sigma_3\lambda_3$ form, which was obtained by *O*-silylation with trimethylsilyl chloride and triethylamine in dry dichloromethane. By using a variation of this method, 1,5-naphthyridine (**6**) was dissolved in dry dichloromethane and 3 equiv. of dimethyl trimethylsilyl phosphite (DMPTMS) were added together with 1 equiv. of sulfuric acid. The mixture was stirred for 5 hours under microwave irradiation (200 W, 45 °C). Analysis by ^{31}P NMR spectroscopy revealed the formation of the double addition product **4** as two diastereoisomers (one major pair of enantiomers, M, and one minor pair of enantiomers, m). An acid–base extraction was used to obtain the envisaged product. The excess phosphite was removed during the acidic extraction by using diethyl ether (dichloromethane cannot be used owing to excessive loss of the end product in the organic phase).

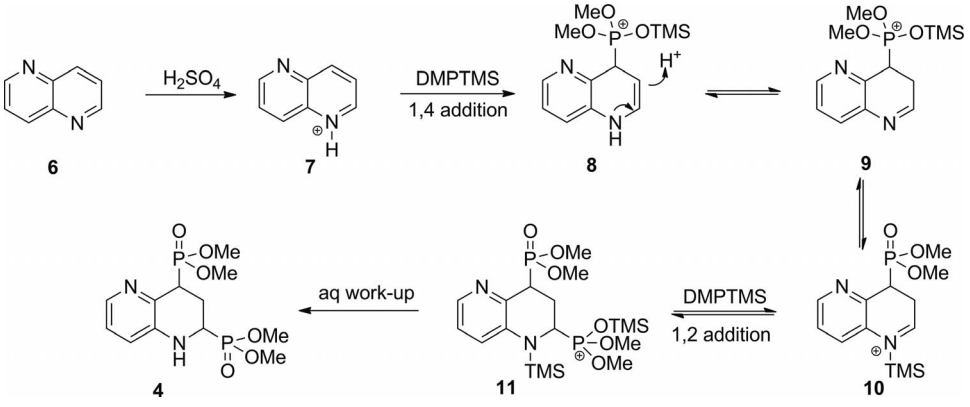

Scheme 1. Proposed mechanism of the tandem 1,4–1,2 addition of DMPTMS to 1,5-naphthyridine.

Table 1. Reaction of different phenanthrolines **5** with dimethyl trimethylsilyl phosphite (DMPTMS) in acidic medium.[a]

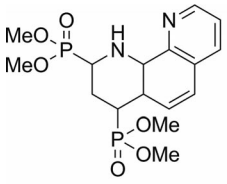

5a (1,10)

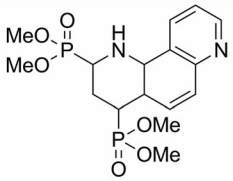

5b (1,7)

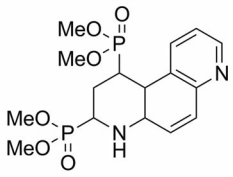

5c (4,7)

Entry	Product **5**	Equiv. DMPTMS	Equiv. H_2SO_4	Time Δ [d]	Time MW [h]	Conversion [%] Δ	Conversion [%] MW	Isolated yield [%] Δ	Isolated yield [%] MW	Ratio M/*m*
1	1,10-	2.05	0.5	5	–	1	–	–	–	–
2	1,7-	2.05	0.5	3	–	0	–	–	–	–
3	4,7-	2.05	0.5	6	–	14	–	–	–	–
4	4,7	4	1	1	–	1	–	–	–	–
5	1,10-	6	1	–	2	–	95	–	88	93:7
6	1,10-	3	0.5	–	3	–	86	–	75	92:8
7	1,10-	3.5	0.5	–	5	–	100	–	96	94:6
8	1,10-	3×1	0.5	–	5	–	62	–	48	95:5
9	1,10-	3×2	3×0.4	–	5	–	26	–	–	–
10	1,7-	3	0.5	–	5	–	67	–	25	>99:1
11	1,7-	3×1	1	–	5	–	35	–	12	98:2
12	1,7-	3×2	3×0.4	–	5	–	20	–	–	–
13	4,7-	6	1	–	3	–	36	–	12	91:9
14	4,7-	3×2	1	–	5	–	22	–	8	90:10
15	4,7-	3×2	3×0.4	–	5	–	15	–	–	–

[a] Δ = reflux, batch; MW = microwave heating (45 °C, 200 W), m = minor diastereomeric pair; M = major diastereomeric pair.

Chromatographic purification was sometimes required to separate the product from the unreacted starting material. Unfortunately, these phosphonylated azaheterocycles, such as diphosphonylated 1,5-naphthyridine **4**, were mainly retained on the column, which led to lower yields than first expected (43% yield in comparison to a 87% conversion; M/m: 87:13). In comparison to the addition of phosphites to quinolines,[10d] 1,5-naphthyridine **4** reacted much slower under the same conditions, and double 1,4-additions were not observed, as protonation of both nitrogen atoms would cause excessive charge in the ring system. To evaluate the scope of the double phosphonylation reaction, 1,10-, 1,7- and 4,7-phenanthroline, which have extended aromatic systems, were evaluated as substrates (Table 1). The double addition was performed under reflux conditions as well as under microwave irradiation. Several derivatives were prepared by using this methodology, and better conversions and yields were established under microwave heating. Thus, it can be concluded that the use of microwave heating is necessary to overcome the activation energy of the aromatic system.

The significant difference in yield between 1,10- and 4,7-phenanthroline highlights the influence of the position of the nitrogen atoms. In an attempt to increase the conversion of 4,7-phenanthroline, the stepwise addition of dimethyl trimethylsilyl phosphite and/or sulfuric acid to reduce the hydrolysis of the silylated phosphite was evaluated (Table 1, Entries 14 and 15). Unfortunately, the addition of the dimethyl trimethylsilyl phosphite in portions to the reaction mixture did not lead to a higher conversion.

2. Theoretical Rationalization of the Reaction Path for Phosphite Addition

A density functional theory (DFT) based computational study was performed (see Computational Details section) to obtain detailed insight into the reaction mechanism and the influence of the substrate on the 1,4–1,2 addition of phosphites. The rate-determining step in the tandem 1,4–1,2 addition of phosphites is known to be the initial 1,4 addition, in which the aromaticity is partially disrupted. 1,4-Addition is initiated by nitrogen protonation, though the ease of attack is governed by the nucleophilic attack of the phosphite species (Scheme 1). Experimentally, quinolines were found to react much faster than naphthyridines and phenanthrolines. Before studying the addition reaction, we investigated the proton affinity, aromaticity and charge distribution of the various substrates. To quantify the aromaticity of the substrates we used the nucleus-independent chemical shift (NICS) values as introduced by Schleyer et al.[12] This parameter has previously been successful in explaining the stability trend of substituted diazanaphthalenes.[13] The free energies of protonation ($\Delta G_{prot,298\ K}$) and the NICS values (in ppm) for all substrates calculated in the plane of the various rings are listed in Table 2.

1,10-Phenanthroline has the highest affinity towards protonation. The difference in the relative stabilities of the phenanthrolines is mainly due to steric features (Figure 3). 1,10-Phenanthroline is energetically less stable than 1,7-phenanthroline and 4,7-phenanthroline. This difference in stability is caused by the position of the nitrogen atoms in

Table 2. Free energies of protonation ($\Delta G_{prot,298\ K}$), activation ($\Delta G_{act,298\ K}$) and reaction free energies ($\Delta G_{r,298\ K}$ and $\Delta G_{rn,298\ K}$) at 298 K. NICS values [ppm] calculated in the plane of the various rings are given. All simulations were performed at the M06-2X/6-31+G(d,p) level of theory.

	Substrate	Protonated substrate	$\Delta G_{prot,298K}$ (kJ/mol)	$\Delta G_{act,298K}$[a] (kJ/mol)	$\Delta G_{r,298K}$[a] (kJ/mol)	$\Delta G_{rn,298K}$[b] (kJ/mol)
Quinoline	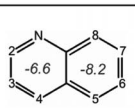	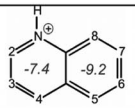	–940	53	–17	–957
1,5-Naphthyridine	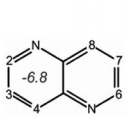	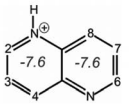	–916	43	–34	–950
1,10-Phenanthroline	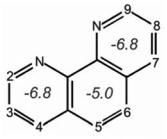	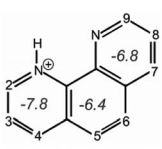	–985	59	4	–981
1,7-Phenanthroline	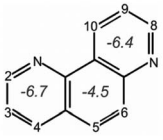	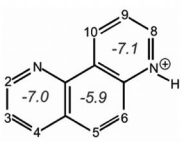 at position N7	–948	47	–23	–903
1,7-Phenanthroline	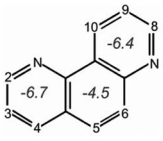	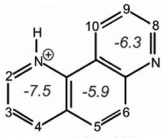 at position N1	–924	53	–7	–931
4,7-Phenanthroline	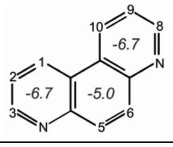	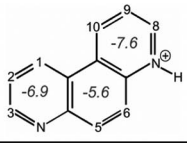	–938	44	–1	–939

[a] Relative to the protonated substrate. [b] Relative to the neutral substrate.

the fused aromatic system. As shown in Figure 3, the nitrogen atoms of 1,10-phenanthroline are relatively close, and hence there is repulsion between their lone pairs. Incidentally, this structural feature brings the protonated form of 1,10-phenanthroline extra stability, as the proton on N1 interacts with the neighbouring nitrogen atom N10, which is relatively close (2.233 Å, Figure 3). The relative Gibbs free energies (G_{rel}) of the protonated forms (Figure 3) reveal N1-protonated 1,10-phenanthroline as the most stable. A low-barrier transition state, in which the proton hops from N1 to N10, has also been located (Figure 4); the ease of tautomerization between the two protonated forms also contributes to the entropic stability of protonated 1,10-phenanthroline. Although 1,10-phenanthroline (C_{2v}) and 4,7-phenanthroline (C_{2v}) both have a C_2 axis of symmetry and, hence, two degenerate (isoelectronic) protonated forms, it is notable that 1,7-phenanthroline (C_s), which only has a plane of symmetry, can have two different protonated states (N1 and N7 protonation) that differ significantly in stability and that protonation of N7 is favoured (Figure 3). It can thus be concluded that 1,7-phenanthroline will be exclusively protonated at the N7 position.

The calculated NICS values show that the bicyclic species are more aromatic than the tricyclic ones, as expected. Quinoline is the most aromatic substrate, followed by naphthyridine and then the phenanthrolines. Protonation at a nitrogen atom increases the aromaticity of the entire aromatic structure and leads to stable pyridinium ions in line with the large proton affinities. The computed NICS value of the protonated ring typically increases from –6.7 to –7.5 ppm, and the NICS values of the fused rings also increase. For the tricyclic species, the energetically favoured 1,10-phenanthroline cation is the most aromatic, followed by the 1,7-phenanthroline protonated at N7 and 4,7-phen-

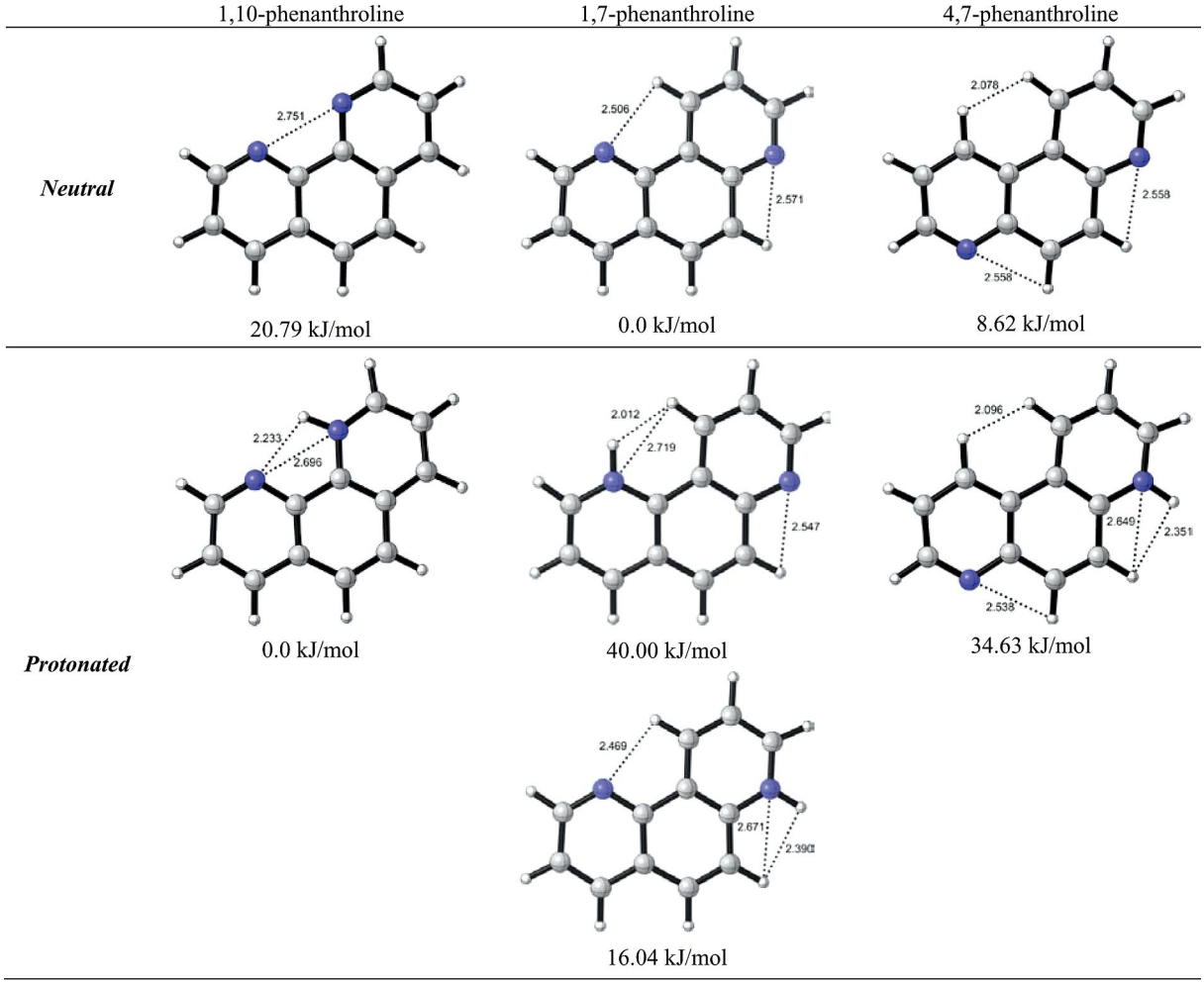

Figure 3. Structures and relative Gibbs free energies (G_{rel}) of neutral and protonated forms of phenanthrolines. M06-2X/6-31+G(d,p) optimized geometries. Selected critical distances given in Å.

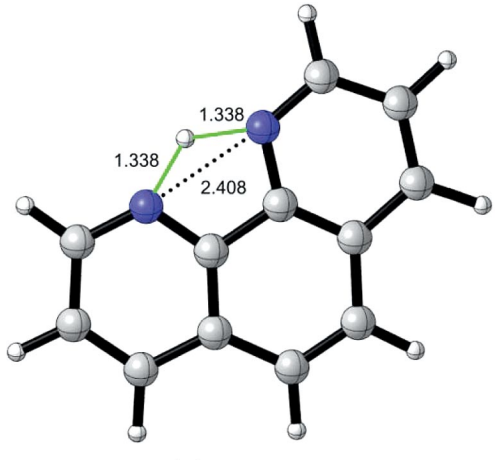

Figure 4. Transition-state structure and Gibbs free energy of activation (ΔG^{taut}) for the low-barrier tautomerization of 1,10-phenanthroline. M06-2X/6-31+G(d,p) optimized geometries. Selected critical distances given in Å.

anthroline cations. The 1,7-phenanthroline protonated at position N1 is the least aromatic. Although the differences are small, this analysis shows that aromaticity is a key factor in the determination of the relative stability of the (protonated) substrates.

As a final step in the analysis of the different proton affinities of the substrates, we calculated charge distributions by using the Hirshfeld-I population scheme on all neutral and protonated compounds.[14] The results are given in Tables S1–S2. Overall, the negative charges on the nitrogen atoms correlate fairly well with the protonation free energies, apart from that for 1,10-phenanthroline, for which the protonated substrate is additionally stabilized by the hydrogen bond N1–H···N10. A correlation plot between the charges on the nitrogen atoms and the proton affinities is shown in Figure 5.

We further investigated the effect of the various substrates and the position of the nitrogen atoms on the activation barriers for phosphite attack. The free energies of activation and reaction free energies at 298 K, starting from the protonated substrates and neutral substrates, are listed in Table 2. Experimentally, quinoline reacted faster than

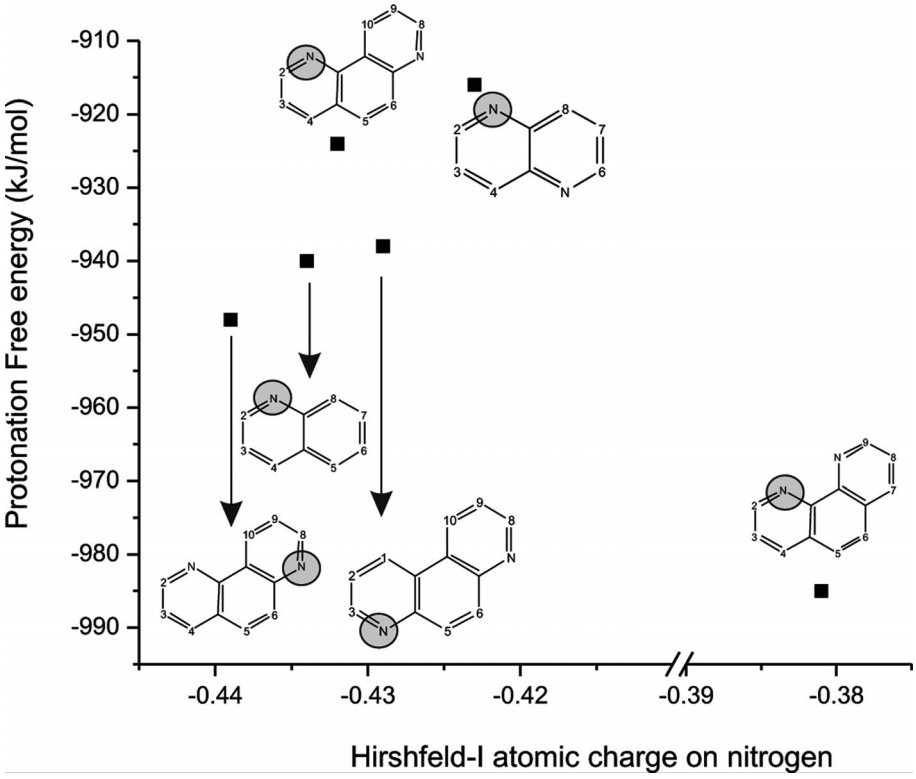

Figure 5. Protonation free energies for quinolines, naphthyridines and phenanthrolines vs. Hirshfeld-I atomic charge on the nitrogen atom of the neutral substrate at the M06-2X/6-31+G(d,p) level of theory.

napthyridine and phenanthrolines. However, it is not possible to compare the energies of the substrates, there is a pronounced difference in protonation energy (–940 vs. –916 kJ/mol). Protonated quinoline is thus more stable than protonated naphthyridine. This indeed results in a higher activation barrier for quinoline: the activation barrier with respect to the protonated substrates are 53 and 43 kJ/mol for quinoline and 1,5-naphthyridine, respectively. However, taking into account both protonation and phosphite addition, the reaction with quinoline is preferred over naphthyridine. Also based on the product stabilities, the addition to quinoline is favoured. The reaction scheme for these two substrates is depicted in Figure 6 (a), and the transition states are given in Figure 7.

Experimentally, a significant difference in product yields was observed when comparing the 1,10- and 4,7-phenanthrolines; this indicates that the position of the nitrogen atoms affects the reactivity. The optimized transition states for the various phenanthrolines are also shown in Figure 7. The variation in the critical distance of the forming P–C bond indicates a difference in synchronicity between the transition states; 4,7-phenanthroline arrives at a later transition state than the others. In all transition-state structures, stabilizing CH–π interactions (2.9–3.2 Å) between the ring

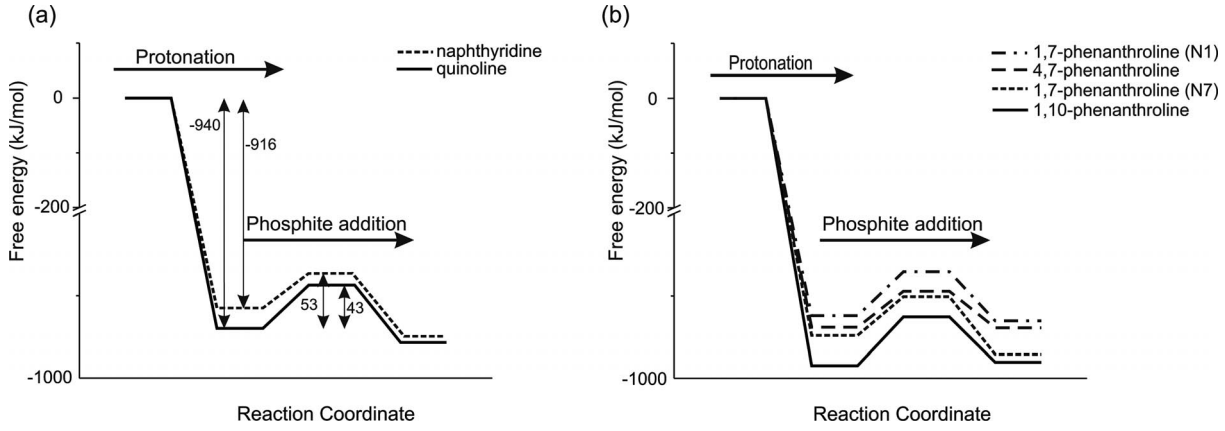

Figure 6. Reaction scheme for phosphite addition to (a) quinoline and naphthyridine and (b) phenanthrolines [at the M06-2X/6-31+G(d,p) level of theory].

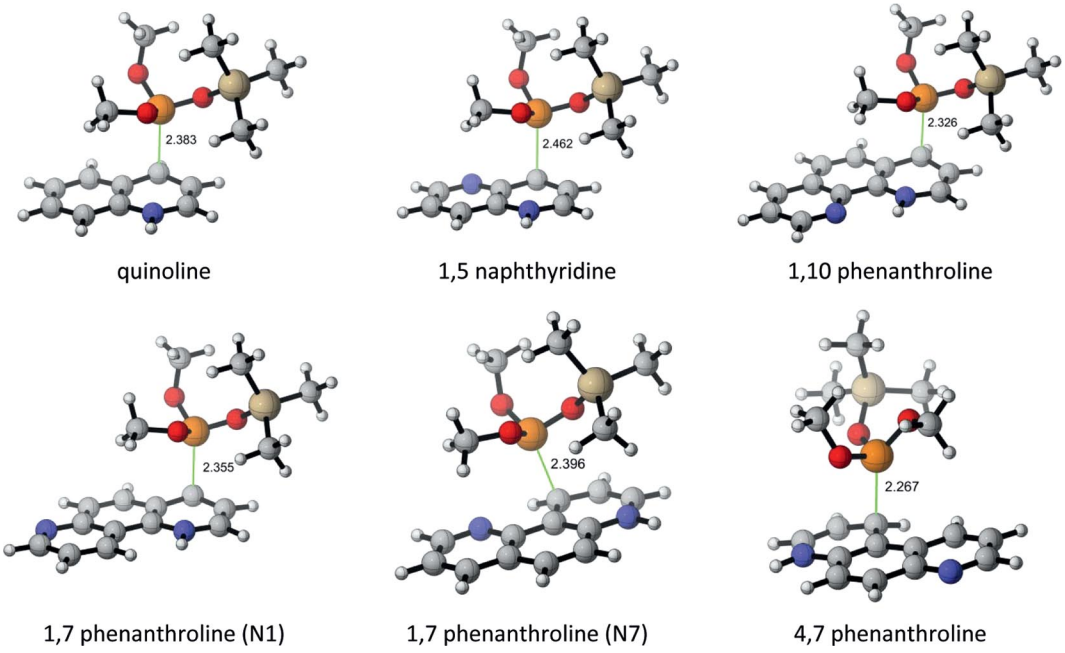

Figure 7. Transition state structures for phosphite attack on quinoline, 1,5-naphthyridine and 1,10-, 1,7- and 4,7-phenanthroline. M06-2X/6-31+G(d,p)-optimized geometries are depicted.

and the phosphite substituents are present. Figure 6 (b) shows the reaction scheme for phosphite attack at the various phenanthrolines. The free-energy scheme is in line with the experimental findings, which yield an overall preference for the phosphite addition at 1,10-phenanthroline. Addition at position N1 of 1,7-phenanthroline is not expected as its proton affinity is smaller than the other phenanthrolines and the intrinsic activation barrier is high.

The product stabilities indicate that the most stable product after attack of the various phenanthrolines corresponds to the 1,10-phenanthroline substrate ($\Delta G_{rn,298\ K}$ in Table 2). As already indicated, 1,10-phenanthroline is relatively unstable owing to repulsion between the nitrogen lone pairs, but upon protonation a stabilizing interaction occurs between the protonated site and the nearby nitrogen atom. This structural feature remains present throughout the reaction cycle. The results of this study indicate the nontrivial effect of the position of heteroatoms in aromatic rings and the prominent effect on their reactivity.

The computed NICS values of the reaction products show that addition of the phosphite totally disrupts the local aromaticity, as positive values are found for all NICS values calculated at the centre of the ring where the addition occurs (see Supporting Information). However, the NICS values of the other rings remain almost unaltered, indicative of the local distortion the addition is causing.

Conclusions

We have shown that our previously described tandem 1,4–1,2 addition of phosphites across imines and quinolines is also applicable to more extended aromatic systems. Despite their lower reactivity in comparison to quinolines, phenanthrolines (1,10; 1,7; 4,7) and 1,5-naphthyridine are appropriate substrates for the syntheses of partially saturated 2,4-diphosphonodiaza heterocycles. To rationalize the observed experimental findings, a thorough molecular modelling study was performed. The intrinsic properties of the various substrates were studied by calculating the proton affinities and the NICS values, which are indicative of aromaticity. Profound differences were found and it was shown that quinoline is the most aromatic substrate, followed by naphthyridine and then the phenanthrolines. Protonation at a nitrogen atom increases the aromaticity of the entire aromatic structure. This is indeed reflected in the protonation free energies of the various substrates and the partial charges on the nitrogen atoms. Protonated quinoline is more stable than protonated naphthyridine. Experimentally, it was found that quinoline reacts much faster than the (poly)cyclic substrates. Theoretical calculations showed that overall the reaction with quinoline is preferred when taking into account both the protonation energy and activation barrier for phosphite addition. When comparing the reactivity of the various phenanthroline substrates, it was found that 1,10-phenanthroline reacts faster than the other substrates and that there is a substantial influence of the particular position of the nitrogen atoms in the phenanthroline substrates. Overall, this study provides a fundamental understanding of the reactivity of 5-naphthyridine and phenanthrolines in the 1,4–1,2 addition of phosphites.

Experimental Section

Microwave Reactions: All microwave reactions were performed in a CEM Discover Focused Microwave Synthesis System with a selectable power output from 0–300 W. The reactions were performed

in 10 mL thick-walled Pyrex reaction vessels closed with a "snap-on" septum cap and equipped with a small stirring bar. The temperature control uses a noncontact infrared sensor to measure the temperature at the bottom of the vessel and is used in a feedback loop with the on-board computer to regulate the temperature from 25–250 °C by adjusting the power output (1 W increments). The pressure control, an IntelliVentTM Pressure Control System, uses an indirect measurement of the pressure by sensing changes in the external deflection of the septum on the top of the sealed pressure vessel. Stirring is performed by a rotating magnetic plate located below the floor of microwave cavity. Cooling of the vessel after the reaction is performed by a stream of clean air onto the vessel, which decreases the temperature of a 2 mL solution from ca. 150 to ca. 40 °C in less than 120 s. A ramp time of maximum 5 min was used, during which the temperature increased from room temperature to the desired one. This temperature was maintained during the course of the reaction for the indicated time.

General Remarks: All reactions were performed with flame-dried glassware and dry solvents under a nitrogen atmosphere. All common reagents and solvents were obtained from commercial suppliers and were used without any further purification unless otherwise noted. High resolution ^{1}H (300 MHz), ^{31}P (121 MHz) and ^{13}C NMR (75 MHz) spectra were recorded with a JEOL EX 300 Eclipse+ NMR spectrometer. Peak assignments were obtained with the aid of DEPT, COSY, heteronuclear single quantum coherence (HSQC) and HMBC spectroscopy. Data are reported as follows: chemical shift, multiplicity (s: singlet, d: doublet, t: triplet, q: quadruplet, br: broad, m: multiplet), coupling constants (*J* in Hz), integration, allocation of the peaks. The compounds were diluted in deuterated solvents, and the solvent used is indicated for each compound. Low resolution mass spectra were recorded with an Agilent 1100 Series VS (ES = 4000 V) mass spectrometer. IR spectra were recorded with a Perkin–Elmer Spectrum BX FTIR spectrometer. All compounds were analyzed in neat form with an attenuated total reflectance (ATR) accessory. The melting points of crystalline compounds were measured with a Büchi 540 apparatus. The elemental analysis was performed with a Perkin–Elmer 2400 elemental analyzer. The purification of reaction mixtures was performed by column chromatography in a glass column with silica gel (Acros, particle size, 0.035–0.070 mm, pore diameter ca. 6 nm). TLC was performed with aluminium backed plates coated with silica gel 60 with F254 indicator (Merck, 0.25 mm) and $KMnO_4$ as a visualizing agent.

Typical Procedure for the Synthesis of Dimethyl Trimethylsilyl Phosphite (DMPTMS): In a flame dried 250 mL flask, dimethyl phosphite (1 equiv., 100 mmol, 11.00 g) was dissolved in dry dichloromethane (150 mL). To this solution was added triethylamine (1.2 equiv., 120 mmol, 12.15 g), after which the solution was stirred at 0 °C under a nitrogen atmosphere. Subsequently, trimethylsilyl chloride (1.1 equiv., 110 mmol, 11.94 g) was added to the solution with a dry syringe. This mixture was stirred for 30 min at 0 °C, and then a sample was taken for ^{31}P NMR spectroscopy. The formed $Et_3N{\cdot}HCl$ salt was removed by filtration, and the solvent was removed in vacuo. The residue was redissolved in dry diethyl ether to precipitate the remaining salt. After filtration and evaporation, the procedure was repeated until there was no more salt formation. The dimethyl trimethylsilyl phosphite was obtained as a colourless liquid with a characteristic smell. It can be stored at –30 °C for a maximum of one month in a well-closed bulb. The yields varied from 70 to 75%. ^{31}P NMR (121 MHz, $CDCl_3$, ppm): δ = 128.51 ppm.

Typical Procedure for the Synthesis of Compounds 4 and 5 (Reflux Conditions): In a dry flask, 1,5-naphthyridine or a phenanthroline derivative (2 mmol) was dissolved in dry dichloromethane together with DMPTMS (3 equiv., 6 mmol, 1.09 g; 3.5 equiv., 7 mmol, 1.28 g; or 6 equiv., 12 mmol, 2.19 g). The mixture was stirred at room temperature under a nitrogen atmosphere, after which sulfuric acid (0.5 equiv., 1 equiv. H^+, 1 mmol, 0.10 g) was added to the solution. The reaction was heated to reflux and was followed by ^{31}P NMR spectroscopy. Whenever possible, conversions were calculated from the integrations in the ^{31}P NMR spectra. An optimized acid–base extraction was used to isolate the end product. After removal of the solvent in vacuo, the residue was redissolved in Et_2O (20 mL) and HCl (3 N, 40 mL). After extraction with diethyl ether (3 × 15 mL), the aqueous phase was neutralized with NaOH (3 N), followed by another extraction with dichloromethane (3 × 20 mL). This second organic phase was dried with $MgSO_4$. After filtration of the solids and removal of the volatiles, the pure end product was obtained in moderate-to-good yields. In some cases, chromatographic purification was required [petroleum ether/ethyl acetate (50:50), followed by acetonitrile/dichloromethane/methanol (80:17:3)]. As the end product exists as two pairs of diastereoisomers, the ratio of the minor and major compound was calculated from ^{31}P NMR spectroscopy. In the following spectra, signals of the minor and major diastereoisomer are indicated with m and M, respectively.

Typical Procedure for the Synthesis of Compounds 4 and 5 (Microwave Heating): In a dry 10 mL thick-walled Pyrex reaction vessel, 1,5-naphthyridine or a phenanthroline derivative (2 mmol) was dissolved in dry dichloromethane (7 mL) together with DMPTMS (3 equiv., 6 mmol, 1.09 g; 3.5 equiv., 7 mmol, 1.28 g; or 6 equiv., 12 mmol, 2.19 g) and sulfuric acid (0.5 equiv., 1 equiv. H^+, 1 mmol, 0.10 g). The head space was flushed with nitrogen before the "snap-on" cap of the tube was closed. The reaction was heated to 45 °C in a microwave synthesis system for 30 min. The progress of the reaction was checked by ^{31}P NMR spectroscopy; a sample was taken directly from the mixture, after which it was again heated to 45 °C for another 30 min. Another sample was taken from the solution to monitor the reaction progress. If this sample revealed the presence of remaining starting material, the reaction mixture was placed back inside the microwave system and was again heated to 45 °C. After complete conversion, the end product was isolated by using the same methodology as that used under reflux conditions. In the case of 4,7-phenanthroline, 6 equiv. DMPTMS were added at once; this is in contrast to the other substrates, for which 3 equiv. were enough to drive the reaction to completion.

Dimethyl [4-(Dimethoxyphosphoryl)-1,2,3,4-tetrahydro-1,5-naphthyridin-2-yl]phosphonate (4): Because of the low quantity of minor isomer (m), only the peaks of the major isomer (M) could be assigned in the ^{13}C NMR spectrum. Minor (m)/major (M) ratio: 13:87. Yellow oil, yield 43%. ^{1}H NMR (300 MHz, $CDCl_3$): δ = 2.11–2.39 (m, 2 H, CH_AH_B, M + m), 2.57–2.71 (m, 2 H, CH_AH_B, M + m), 3.62 (dtd, $^{2}J_{H,P}$ = 24.8, *J* = 5.5, 2.2 Hz, 2 H, C*H*P, M + m), 3.66 [d, $^{3}J_{H,P}$ = 10.5 Hz, 3 H, P(O)OCH_3, M], 3.78 [d, $^{3}J_{H,P}$ = 10.5 Hz, 3 H, P(O)OCH_3, m], 3.80 [d, $^{3}J_{H,P}$ = 11.0 Hz, 3 H, P(O)OCH_3, M], 3.84 [d, $^{3}J_{H,P}$ = 10.5 Hz, 9 H, 3 × P(O)OCH_3, 2 × M + m], 3.87 [d, $^{3}J_{H,P}$ = 10.5 Hz, 3 H, P(O)OCH_3, m], 3.93 [d, $^{3}J_{H,P}$ = 11.0 Hz, 3 H, P(O)OCH_3, m], 4.26 (ddd, $^{2}J_{H,P}$ = 11.8, *J* = 7.7, 3.3 Hz, 1 H, NC*H*P, M), 4.31–4.36 (m, 1 H, NC*H*P, m), 4.48 (br. s, 1 H, N*H*, M), 4.55 (br. s, 1 H, N*H*, m), 6.88 (m, 1 H, 8-H, m), 6.92 (dd, *J* = 8.3, 1.1 Hz, 1 H, 8-H, M), 6.99 (dd, *J* = 4.4, 2.2 Hz, 1 H, 7-H, M), 7.01 (dd, *J* = 4.4, *J* = 2.2 Hz, 1 H, 7-H, m), 7.98 (dd, *J* = 4.4, 1.1 Hz, 1 H, 6-H, M), 8.03 (dd, *J* = 4.4, 1.1 Hz, 1 H, 6-H, m) ppm. ^{13}C NMR (75 MHz, $CDCl_3$): δ = 22.37 (t, *J* = 4.6 Hz, CH*C*H_2CH), 37.45 (dd, $^{1}J_{C,P}$ = 139.0, $^{3}J_{C,P}$ = 15.0 Hz, *C*HP), 45.29 (d, $^{1}J_{C,P}$ = 161.5 Hz, N*C*HP), 52.86 [d, $^{2}J_{C,P}$ = 6.9 Hz,

P(O)OCH$_3$], 53.18 [d, $^2J_{C,P}$ = 6.9 Hz, P(O)OCH$_3$], 53.59 [d, $^2J_{C,P}$ = 6.9 Hz, P(O)OCH$_3$], 53.88 [d, $^2J_{C,P}$ = 6.9 Hz, P(O)OCH$_3$], 122.18 (s, C-8), 123.33 (d, *J* = 3.5 Hz, C-7), 135.21 (d, *J* = 8.1 Hz, C-4a), 139.12 (d, *J* = 2.3 Hz, C-6), 139.97 (dd, *J* = 12.1, 4.6 Hz, C-8a) ppm. ^{31}P NMR (121 MHz, CDCl$_3$): δ = 26.11 (d, $J_{P,P}$ = 13.4 Hz, m), 27.24 (d, $J_{P,P}$ = 2.2 Hz, M), 28.87 (d, $J_{P,P}$ = 2.2 Hz, M), 30.18 (d, $J_{P,P}$ = 13.4 Hz, m) ppm. IR: $\tilde{\nu}_{max}$ = 3290 (NH), 1586 [CH(Ar)], 1458 [CH(Ar)], 1229 [CH(Ar)], 1228 (P=O), 1023 (P–O) cm^{-1}. MS (ESI): *m*/*z* (%) = 351.2 (100) [M + H]$^+$. Chromatography: CH$_3$CN/CH$_2$Cl$_2$/MeOH (80:17:3) R_f = 0.06 (M).

Dimethyl [4-(Dimethoxyphosphoryl)-1,2,3,4-tetrahydro-1,10-phenanthrolin-2-yl]phosphonate (5a): Because of the low quantity of minor isomer (m), only the peaks of the major isomer (M) could be assigned in the ^{13}C NMR spectrum. Minor (m)/major (M) ration: 6:94. Orange oil, yield 96%. ^{1}H NMR (300 MHz, CDCl$_3$): δ = 2.15–2.42 (m, 2 H, CH$_A$H$_B$, M + m), 2.63–2.75 (m, 2 H, CH$_A$H$_B$, M + m), 3.54 (dtd, $^2J_{H,P}$ = 23.7, *J* = 5.2, 1.7 Hz, 2 H, CHP, M + m), 3.65 [d, $^3J_{H,P}$ = 10.5 Hz, 3 H, P(O)OCH$_3$, M], 3.66 [d, $^3J_{H,P}$ = 10.5 Hz, 3 H, P(O)OCH$_3$, m], 3.68 [d, $^3J_{H,P}$ = 10.5 Hz, 6 H, P(O)-OCH$_3$, M + m], 3.88 [d, $^3J_{H,P}$ = 10.5 Hz, 6 H, P(O)OCH$_3$, M + m], 3.89 [d, $^3J_{H,P}$ = 10.5 Hz, 3 H, P(O)OCH$_3$, M], 3.90 [d, $^3J_{H,P}$ = 10.5 Hz, 3 H, P(O)OCH$_3$, m], 4.32 (ddd, *J* = 11.7, 8.3, 3.3 Hz, 2 H, NCHP, M + m), 6.53 (d, *J* = 4.4 Hz, 1 H, NH, M), 6.71 (d, *J* = 13.2 Hz, NH, m), 7.06 (d, *J* = 8.3 Hz, 1 H, 6-H, M), 7.14 (d, *J* = 8.8 Hz, 1 H, 6-H, m), 7.34 (d, *J* = 7.7 Hz, 2 H, 8-H, M + m), 7.36 (dd, *J* = 8.3, *J* = 1.7 Hz, 2 H, 5-H, M + m), 8.01 (dd, *J* = 8.3, 1.7 Hz, 2 H, 7-H, M + m), 8.72 (dd, *J* = 3.9, 1.7 Hz, 2 H, 9-H, M + m) ppm. ^{13}C NMR (75 MHz, CDCl$_3$): δ = 22.03 (t, $^2J_{C,P}$ = 4.6 Hz, CHCH$_2$CH), 34.43 (dd, $^1J_{C,P}$ = 141.9, $^3J_{C,P}$ = 15.0 Hz, CHP), 45.13 (d, $^1J_{C,P}$ = 159.2 Hz, NCHP), 53.13 [d, $^2J_{C,P}$ = 6.9 Hz, P(O)OCH$_3$], 53.33 [d, $^2J_{C,P}$ = 6.9 Hz, P(O)OCH$_3$], 53.39 [d, $^2J_{C,P}$ = 6.9 Hz, P(O)OCH$_3$], 53.68 [d, $^2J_{C,P}$ = 6.9 Hz, P(O)OCH$_3$], 108.37 (d, *J* = 6.9 Hz, C-4a), 114.36 (d, *J* = 2.3 Hz, C-6), 121.52 (s, C-8), 127.87 (s, C-6a), 129.11 (d, *J* = 3.5 Hz, C-5), 135.73 (s, C-7), 137.57 (d, *J* = 2.3 Hz, C-10a), 139.86 (dd, *J* = 10.4, 6.9 Hz, C-10b), 147.47 (s, C-9) ppm. ^{31}P NMR (121 MHz, CDCl$_3$): δ = 26.62 (d, $J_{P,P}$ = 11.9 Hz, m), 27.59 (d, $J_{P,P}$ = 2.2 Hz, M), 29.43 (d, $J_{P,P}$ = 2.2 Hz, M), 30.47 (d, $J_{P,P}$ = 11.9 Hz, m) ppm. IR: $\tilde{\nu}_{max}$ = 3397 (NH), 1571 [CH(Ar)], 1512 [CH(Ar)], 1478 [CH(Ar)], 1232 (P=O), 1016 (P–O) cm^{-1}. MS (ESI): *m*/*z* (%) = 401.2 (100) [M + H]$^+$. Chromatography: CH$_3$CN/CH$_2$Cl$_2$/MeOH (80:17:3) R_f = 0.14 (M + m).

Dimethyl [4-(Dimethoxyphosphoryl)-1,2,3,4-tetrahydro-1,7-phenanthrolin-2-yl]phosphonate (5b): Because of the low quantity of minor isomer (m), only the peaks of the major isomer (M) could be assigned in the ^{1}H and ^{13}C NMR spectrum. Minor (m)/major (M) ration: < 1:99. Yellow powder, yield 25%, m.p. 157–159 °C. C$_{16}$H$_{24}$N$_2$O$_6$P$_2$ (402.32): calcd. C 47.77, H 6.01, N 6.96 ; found C 47.91, H 5.45, N 6.73. ^{1}H NMR (300 MHz, CDCl$_3$): δ = 2.01–2.29 (m, 1 H, CH$_A$H$_B$), 2.75 (td, *J* = 11.3, 1.7 Hz, 1 H, CH$_A$H$_B$), 3.33 [d, $^3J_{H,P}$ = 10.5 Hz, 3 H, P(O)OCH$_3$], 3.80 [d, $^3J_{H,P}$ = 10.5 Hz, 3 H, P(O)OCH$_3$], 3.83 [d, $^3J_{H,P}$ = 10.5 Hz, 3 H, P(O)OCH$_3$], 3.85 [d, $^3J_{H,P}$ = 10.5 Hz, 3 H, P(O)OCH$_3$], 4.49 (ddd, *J* = 12.3, 7.2, 4.4 Hz, 1 H, NCHP), 4.77 (ddt, $^2J_{H,P}$ = 23.7, *J* = 5.5, 1.7 Hz, 1 H, CHP), 4.98 (d, *J* = 3.9 Hz, 1 H, NH), 6.93 (d, *J* = 8.8 Hz, 1 H, 6-H), 7.13 (dd, *J* = 8.8, 4.4 Hz, 1 H, H-9), 7.49 (dd, *J* = 8.8, 2.2 Hz, 1 H, 5-H), 7.92 (dd, *J* = 8.3, 1.7 Hz, 1 H, 10-H), 8.79 (dd, *J* = 4.4, 1.7 Hz, 1 H, 8-H) ppm. ^{13}C NMR (75 MHz, CDCl$_3$): δ = 22.03 (s, CHCH$_2$CH), 28.68 (dd, $^1J_{C,P}$ = 141.3, $^3J_{C,P}$ = 15.0 Hz, CHP), 45.73 (d, $^1J_{C,P}$ = 158.1 Hz, NCHP), 52.88 [d, $^2J_{C,P}$ = 6.9 Hz, P(O)OCH$_3$], 52.93 [d, $^2J_{C,P}$ = 6.9 Hz, P(O)OCH$_3$], 53.19 [d, $^2J_{C,P}$ = 6.9 Hz, P(O)OCH$_3$], 53.86 [d, $^2J_{C,P}$ = 6.9 Hz, P(O)OCH$_3$], 106.06 (d, *J* = 6.9 Hz, C-10a), 117.39 (s, C-9), 118.74 (d, *J* = 3.5 Hz, C-6), 122.05 (s, C-4a), 127.92 (d, *J* = 3.5 Hz, C-5), 135.82 (s, C-10), 144.02 (dd, *J* = 9.2, 5.8 Hz, C-10b), 147.17 (d, *J* = 4.6 Hz, C-6a), 149.41 (s, C-8] ppm. ^{31}P NMR (121 MHz, CDCl$_3$): δ = 28.02 (s, M), 30.55 (s, M) ppm. IR: $\tilde{\nu}_{max}$ = 3294 (NH), 1619 [CH(Ar)], 1537 [CH(Ar)], 1432 [CH(Ar)], 1228 (P=O), 1012 (P–O) cm^{-1}. MS (ESI): *m*/*z* (%) = 401.2 (100) [M + H]$^+$. Chromatography: CH$_3$CN/CH$_2$Cl$_2$/MeOH (80:17:3) R_f = 0.05 (M).

Dimethyl [4-(Dimethoxyphosphoryl)-1,2,3,4-tetrahydro-4,7-phenanthrolin-2-yl]phosphonate (5c): Minor (m)/major (M) ratio: 9:91. Orange oil, yield 12%. ^{1}H NMR (300 MHz, CDCl$_3$): δ = 2.02–2.33 (m, 1 H, CHCH$_A$H$_B$CH, M), 2.37–2.51 (m, 1 H, CHCH$_A$H$_B$CH, m), 2.66–2.79 (m, 1 H, CHCH$_A$H$_B$CH, M), 2.81–2.94 (m, 1 H, CHCH$_A$H$_B$CH, m), 3.39 [d, $^3J_{H,P}$ = 10.5 Hz, 3 H, P(O)OCH$_3$, M], 3.57 [d, $^3J_{H,P}$ = 10.5 Hz, 3 H, P(O)OCH$_3$, m], 3.63 [d, $^3J_{H,P}$ = 10.5 Hz, 3 H, P(O)OCH$_3$, M], 3.79 [d, $^3J_{H,P}$ = 10.5 Hz, 3 H, P(O)OCH$_3$, m], 3.86 [d, $^3J_{H,P}$ = 10.5 Hz, 6 H, 2× P(O)OCH$_3$, M], 3.88 [d, $^3J_{H,P}$ = 10.5 Hz, 3 H, P(O)OCH$_3$, m], 3.91 [d, $^3J_{H,P}$ = 10.5 Hz, 3 H, P(O)OCH$_3$, m], 3.94–4.06 (m, 2 H, CHP, M + m), 4.44 (ddd, $^2J_{H,P}$ = 12.5, *J* = 7.2, 3.9 Hz, 2 H, NCHP, M + m), 4.77 (d, *J* = 4.4 Hz, 2 H, NH, M + m), 7.07 (d, *J* = 9.4 Hz, 1 H, 5-H, M), 7.18 (d, *J* = 8.8 Hz, 1 H, 9-H, m), 7.35 (dd, *J* = 8.8, 4.4 Hz, 1 H, 9-H, M), 7.40 (d, *J* = 9.4 Hz, 1 H, 5-H, m), 7.83 (dd, *J* = 9.4, 2.2 Hz, 1 H, 6-H, M), 7.94 (dd, *J* = 9.4, 2.2 Hz, 1 H, 6-H, m), 8.24 (d, *J* = 8.8 Hz, 1 H, 10-H, M), 8.39 (d, *J* = 8.3 Hz, 1 H, 10-H, m), 8.64 (d, *J* = 3.9 Hz, 1 H, 8-H, M), 8.69 (d, *J* = 3.9 Hz, 1 H, 8-H, m) ppm. ^{13}C NMR (75 MHz, CDCl$_3$): δ = 22.25 (t, $^2J_{C,P}$ = 4.6 Hz, CHCH$_2$CH, M), 27.38 (d, $^2J_{C,P}$ = 3.5 Hz, CHCH$_2$CH, m), 30.46 (dd, $^1J_{C,P}$ = 147.7, $^3J_{C,P}$ = 12.7 Hz, CHP, m), 30.59 (dd, $^1J_{C,P}$ = 143.1, $^3J_{C,P}$ = 15.0 Hz, CHP, M), 45.41 (d, $^1J_{C,P}$ = 159.2 Hz, NCHP, M), 52.68 [d, $^2J_{C,P}$ = 6.9 Hz, P(O)OCH$_3$, m], 52.89 [d, $^2J_{C,P}$ = 6.9 Hz, P(O)OCH$_3$, m], 53.09 [d, $^2J_{C,P}$ = 6.9 Hz, 2× P(O)OCH$_3$, M], 53.26 [d, $^2J_{C,P}$ = 6.9 Hz, P(O)OCH$_3$, M], 53.71 [d, $^2J_{C,P}$ = 6.9 Hz, P(O)OCH$_3$, m], 53.76 [d, $^2J_{C,P}$ = 6.9 Hz, P(O)OCH$_3$, m], 53.91 [d, $^2J_{C,P}$ = 6.9 Hz, P(O)OCH$_3$, M], 54.80 (d, *J* = 163.8 Hz, NCHP, m), 102.85 (d, *J* = 6.9 Hz, C-10b, M), 110.75 (d, *J* = 6.9 Hz, C-10b, m), 121.24 (s, C-9, M), 121.44 (s, C-9, m), 121.62 (d, *J* = 3.5 Hz, C-5, M), 122.66 (d, *J* = 4.6 Hz, C-5, m), 128.05 (d, *J* = 3.5 Hz, C-10a, M), 129.82 (d, *J* = 3.5 Hz, C-10a, m), 130.05 (s, C-10, m), 130.24 (s, C-10, M), 130.36 (d, *J* = 3.5 Hz, C-6, m), 130.47 (d, *J* = 3.5 Hz, C-6, M), 141.28 (dd, *J* = 9.2, 5.8 Hz, C-4a, M), 143.34 (s, C-6a, m), 143.60 (d, *J* = 2.3 Hz, C-6a, M), 145.73 (t, *J* = 5.8 Hz, C-4a, m), 146.01 (s, C-8, M), 146.88 (s, C-8, m) ppm. ^{31}P NMR (121 MHz, CDCl$_3$): δ = 26.84 (s, m), 27.52 (s, M), 28.35 (s, m), 28.88 (s, M) ppm. IR: $\tilde{\nu}_{max}$ = 3294 (NH), 1618 [CH(Ar)], 1525 [CH(Ar)], 1477 [CH(Ar)], 1230 (P=O), 1024 (P–O) cm^{-1}. MS (ESI): *m*/*z* (%) = 401.2 (100) [M + H]$^+$. Chromatography: CH$_2$Cl$_2$/MeOH (95:5) R_f = 0.10 (M + m).

Computational Details: All computations were performed with the Gaussian 09 program package.[15] Geometry optimizations were carried out by using the M06-2X functional,[16] which is known to perform well in organic systems with dispersion effects.[17] The nature of the stationary points was confirmed by normal modes analysis. Free energy corrections are reported at 1 atm and 298 K. The HiPart[18] program was used to compute Iterative Hirshfeld (Hirshfeld-I) charges,[14] which are known to reliably reproduce electrostatic potential surfaces (ESP).[19] Furthermore, it was recently shown that Hirshfeld-I charges are basis-set independent[20] and robust with respect to conformational changes in organic[21] and biological systems.[22] NICS values were calculated in the plane of each six-membered ring by using the default gauge-independent atomic orbital (GIAO) method.[23] NICS values are reported to be relatively insensitive to the level of theory employed, as stated by Chen et al.[12b]

Supporting Information (see footnote on the first page of this article): ^{1}H and ^{13}C NMR spectra of **4**, **5a**, **5b** and **5c**; Hirshfeld-I charges for the neutral and *N*-protonated forms of quinoline and 1,5-naphthyridine (Table S1) and 1,10-, 1,7- and 4,7-phenanthroline (Table S2); NICS values of the products (Figure S1).

Acknowledgments

The Research Board of Ghent University (BOF) and the Flemish Research Foundation (FWO) are acknowledged for financial support. Financial support was also received from BELSPO in the frame of IAP/7/05. The computational resources used in this work were provided by Stevin Supercomputer Infrastructure, Ghent University.

[1] K. Moonen, I. Laureyn, C. V. Stevens, *Chem. Rev.* **2004**, *104*, 6177.

[2] a) D. Redmore, *US Pat.* 3 673 196, **1972** [*Chem. Abstr.* **1972**, *77*, 88653p]; b) D. Redmore, *US Pat.* 3 775 057, **1973** [*Chem. Abstr.* **1974**, *80*, 147521]; c) D. Redmore, *US Pat.* 3 786 055, **1974** [*Chem. Abstr.* **1974**, *80*, 96154]; d) D. Redmore, *US Pat.* 3 888 627, **1975** [*Chem. Abstr.* **1975**, *83*, 97570k]; e) D. Redmore, *US Pat.* 3 810 907, **1974** [*Chem. Abstr.* **1974**, *81*, 37646].

[3] a) G. V. Protopopova, L. I. Reidalova, A. F. Pavlenko, L. S. Sologub, V. P. Kukhar, V. S. Petrenko, *Fiziol. Akt. Veshchestva* **1980**, *12*, 16–18; b) V. P. Kukhar, T. I. Cherepenko, A. F. Pavlenko, *Dokl. Akad. Nauk Ukr. RSR., Ser. B: Geol. Khim. Biol. Nauki* **1982**, *12*, 60–63; c) K. Akiba and K. Tsuzuki, *Jpn. Kokai Tokkyo Koho*, 61 221 102, **1986**; d) S. K. Malhotra, I. L. Evoy, *US Pat.* 4 606 757, **1986** [*Chem. Abstr.* **1987**, *106*, 50053].

[4] a) K. J. Murray, R. A. Porter, H. D. Prain, B. H. Warrington, *PCT Int. Appl.*, 9 117 987, **1991** [*Chem. Abstr.* **1992**, *117*, 48568]; b) T. Johansson, A. Kers, J. Stawinski, *Tetrahedron Lett.* **2001**, *42*, 2217–2220.

[5] a) D. Redmore, *J. Org. Chem.* **1969**, *34*, 1420–1425; b) B. C. Saunders, P. Simpson, *J. Chem. Soc.* **1963**, 3351–3360; c) D. Seyferth, J. D. H. Paetsch, *J. Org. Chem.* **1969**, *34*, 1483–1484; d) M. Regitz, W. Anschütz, A. Liedhegener, *Chem. Ber.* **1968**, *101*, 3734–3743; e) C. E. Griffin, R. P. Peller, J. A. Peters, *J. Org. Chem.* **1965**, *30*, 91–96; f) D. Redmore, *Chem. Rev.* **1971**, *71*, 315–337; g) G. M. Kosolapoff, C. H. Roy, *J. Org. Chem.* **1961**, *26*, 1895–1898; h) A. Burger, J. B. Clements, N. D. Dawson, R. B. Henderson, *J. Org. Chem.* **1955**, *20*, 1383–1386; i) S. Van der Jeught, C. V. Stevens, *Chem. Rev.* **2009**, *109*, 2672–2702.

[6] a) I. Takeuchi, Y. Hamada, K. Hatano, Y. Kurono, T. Yashiro, *Chem. Pharm. Bull.* **1990**, *38*, 1504–1505; b) H. Suezawa, M. Hirota, Y. Shibata, I. Takeuchi, Y. Hamada, *Bull. Chem. Soc. Jpn.* **1986**, *59*, 2362–2364; c) Y. Shibata, I. Takeuchi, Y. Hamada, *Yakugaku Zasshi* **1987**, *107*, 945–953.

[7] J. Barycki, R. Gancarz, M. Milewska, R. Tyka, W. Sawka-Dobrowolska, *Phosphorus Sulfur Silicon Relat. Elem.* **1998**, *143*, 167–178.

[8] I. Takeuchi, Y. Shibata, Y. Hamada, *Heterocycles* **1985**, *23*, 1635–1638.

[9] a) I. Takeuchi, Y. Hamada, *Heterocycles* **1991**, *32*, 261–268; b) I. Takeuchi, Y. Shibata, Y. Hamada, M. Kido, *Heterocycles* **1986**, *24*, 647–650; c) K. Ishikawa, K. Akiba, N. Inamoto, *Synthesis* **1978**, 608.

[10] a) K. Moonen, E. Van Meenen, A. Verwée, C. V. Stevens, *Angew. Chem.* **2005**, *117*, 7573; *Angew. Chem. Int. Ed.* **2005**, *44*, 7407–7411; b) E. Van Meenen, K. Moonen, A. Verwée, C. V. Stevens, *J. Org. Chem.* **2006**, *71*, 7903–7906; c) C. V. Stevens, E. Van Meenen, K. G. R. Masschelein, K. Moonen, A. De Blieck, J. Drabowicz, *Synlett* **2007**, 2549–2552; d) A. De Blieck, K. G. R. Masschelein, F. Dhaene, E. Rozycka-Sokolowska, B. Marciniak, J. Drabowicz, C. V. Stevens, *Chem. Commun.* **2010**, *46*, 258–260.

[11] K. Afarinkia, C. W. Rees, J. I. G. Cadogan, *Tetrahedron* **1990**, *46*, 7175–7196.

[12] a) P. v. R. Schleyer, C. Maerker, A. Dransfeld, H. J. Jiao, N. Hommes, *J. Am. Chem. Soc.* **1996**, *118*, 6317; b) Z. Chen, C. S. Wannere, C. Corminboeuf, R. Puchta, P. v. R. Schleyer, *Chem. Rev.* **2005**, *105*, 3842.

[13] S. Gümüs, *Comput. Theor. Chem.* **2011**, *963*, 263–267.

[14] P. Bultinck, C. Van Alsenoy, P. W. Ayers, C. Ramon, *J. Chem. Phys.* **2007**, *126*, 144111–144112.

[15] M. J. Frisch, G. W. Trucks, H. B. Schlegel, G. E. Scuseria, M. A. Robb, J. R. Cheeseman, J. A. Montgomery, T. V. Jr., K. N. Kudin, J. C. Burant, J. M. Millam, S. S. Iyengar, J. Tomasi, V. Barone, B. Mennucci, M. Cossi, G. Scalmani, N. Rega, G. A. Petersson, H. Nakatsuji, M. Hada, M. Ehara, K. Toyota, R. Fukuda, J. Hasegawa, M. Ishida, T. Nakajima, Y. Honda, O. Kitao, H. Nakai, M. Klene, X. Li, J. E. Knox, H. P. Hratchian, J. B. Cross, V. Bakken, C. Adamo, J. Jaramillo, R. Gomperts, R. E. Stratmann, O. Yazyev, A. J. Austin, R. Cammi, C. Pomelli, J. W. Ochterski, P. Y. Ayala, K. Morokuma, G. A. Voth, P. Salvador, J. J. Dannenberg, V. G. Zakrzewski, S. Dapprich, A. D. Daniels, M. C. Strain, O. Farkas, D. K. Malick, A. D. Rabuck, K. Raghavachari, J. B. Foresman, J. V. Ortiz, Q. Cui, A. G. Baboul, S. Clifford, J. Cioslowski, B. B. Stefanov, G. Liu, A. Liashenko, P. Piskorz, I. Komaromi, R. L. Martin, D. J. Fox, T. Keith, M. A. Al-Laham, C. Y. Peng, A. Nanayakkara, M. Challacombe, P. M. W. Gill, B. Johnson, W. Chen, M. W. Wong, C. Gonzalez, J. A. Pople, *Gaussian 09*, rev. A.1, Gaussian, Inc., Wallingford CT, **2009**.

[16] Y. Zhao, D. G. Truhlar, *Theor. Chem. Acc.* **2008**, *120*, 215.

[17] a) L. Liu, D. Malhotra, R. S. Paton, K. N. Houk, G. B. Hammond, *Angew. Chem. Int. Ed.* **2010**, *49*, 9132; b) S. Catak, M. D'hooghe, N. De Kimpe, M. Waroquier, V. Van Speybroeck, *J. Org. Chem.* **2010**, *75*, 885; c) S. Catak, K. Hemelsoet, L. Hermosilla, M. Waroquier, V. Van Speybroeck, *Chem. Eur. J.* **2011**, *17*, 12027; d) J. M. Winne, S. Catak, M. Waroquier, V. Van Speybroeck, *Angew. Chem. Int. Ed.* **2011**, *50*, 11990; e) K. Mollet, S. Catak, M. Waroquier, V. Van Speybroeck, M. D'hooghe, N. De Kimpe, *J. Org. Chem.* **2011**, *76*, 8364.

[18] T. Verstraelen, *HiPart: A Hirshfeld partitioning program*, Center for Molecular Modeling, Ghent University, **2010**; http://molmod.ugent.be/code.

[19] T. Verstraelen, V. Van Speybroeck, M. Waroquier, *J. Chem. Phys.* **2009**, *131*, 044127.

[20] P. Bultinck, P. W. Ayers, S. Fias, K. Tiels, C. Van Alsenoy, *Chem. Phys. Lett.* **2007**, *444*, 205.

[21] S. Catak, M. D'hooghe, T. Verstraelen, K. Hemelsoet, A. Van Nieuwenhove, H. J. Ha, M. Waroquier, N. De Kimpe, V. Van Speybroeck, *J. Org. Chem.* **2010**, *75*, 4530.

[22] a) T. Verstraelen, E. Pauwels, F. De Proft, V. Van Speybroeck, P. Geerlings, M. Waroquier, *J. Chem. Theory Comput.* **2012**, *8*, 661; b) B. K. Mishra, J. S. Arey, N. J. Sathyamurthy, *Phys. Chem. A* **2010**, *114*, 9606.

[23] J. R. Cheeseman, G. W. Trucks, T. A. Keith, M. J. Frisch, *J. Chem. Phys.* **1996**, *104*, 5497–509, and references cited therein.

Received: October 28, 2012
Published Online: January 14, 2013

